Supporting Information

Two-Dimensional $(PEA)_2PbBr_4$ Perovskite Single Crystals for High Performance UV-Detector

Yunxia Zhang[a#], Yucheng Liu[a#], Zhuo Xu[a], Haochen Ye[a], Qingxian Li[a], Mingxin Hu[a], Zhou Yang[a], Shengzhong (Frank) Liu [a,b*]*

[a]Key Laboratory of Applied Surface and Colloid Chemistry, Ministry of Education; Shaanxi Key Laboratory for Advanced Energy Devices; Shaanxi Engineering Lab for Advanced Energy Technology; Institute for Advanced Energy Materials; School of Materials Science and Engineering, Shaanxi Normal University, Xi'an 710119, China.

[b]iChEM, Dalian National Laboratory for Clean Energy; Dalian Institute of Chemical Physics, Chinese Academy of Sciences, Dalian, 116023, China.

*e-mail: szliu@dicp.ac.cn; zyang@snnu.edu.cn

Experimental Section

Materials: N, N-dimethylformamide (DMF, 99.9%) and Lead bromide ($PbBr_2$, 99%) were purchased from Aladdin Reagent Ltd. Phenylethylammonium bromid (PEABr, 99%) was purchased from Xi'an Polymer Light Technology Corp. All the chemicals were used as received without further purification.

Synthesis of $(PEA)_2PbBr_4$ single crystals: the growth procedure is schematically illustrated in Figure 2a with a facile solvent evaporation method. Briefly, 1.835 g $PbBr_2$ and 2.01 g PEABr are dissolved in 4.4 ml DMF at room temperature under stirring to yield 0.873 g/mL $(PEA)_2PbBr_4$ precursor solution. After filtration, a transparent solution was produced. The filtrated precursor solution was stored in a beaker sealed with wrap containing 4 holes at room temperature (23 ± 0.5 ^oC). After several days, the desired $(PEA)_2PbBr_4$ single crystals with a size of centimeters were obtained.

Characterizations: XRD measurements were performed using Rigaku (Smartlab-9kW) X-ray diffractometer equipped with a Cu Kα X-ray (λ = 1.54186 Å) tube operated at 40 kV and 30 mA. The SEM image were collected with a field emission scanning electron microscopy (FE-SEM; SU-8020, Hitachi). The absorption spectra were measured using a Perkin-Elmer Lambda 950 UV-Vis-NIR spectrophotometer in transmission mode with an integrating sphere attachment operating in the 300~800 nm region. The ultraviolet photoelectron spectroscopy was performed with a photoelectron spectrometer (ESCALAB 250Xi, Thermo Fisher Scientific). The steady-state and time resolved photoluminescence measurement were obtained using a PicoQuant FT-300 and MT-100. The Fluorescence quantum yields were determined by Quantaurus-QY

(Hamamatsu Photonics). Thermogravimetric analysis (TGA) was performed on a TA SDT-Q600 V20.9 (Build 20). The sample was placed in an Al_2O_3 crucible and heated in an interval from room temperature to 800 °C at a ramp rate 10 °C min^{-1} under flowing nitrogen gas. Approximately 5 mg of $(PEA)_2PbBr_4$ single crystal powder was used for experiment.

Computational details: In our calculations, the plane wave method in the framework of density-functional theory (DFT) as implemented in the VASP code is employed.[1,2] The projector augmented wave method is used to describe the interaction between ion-cores and valence electrons.[3] The generalized gradient approximation (GGA) with the Perdew Burke Ernzerhof (PBE) functional is used for the exchange-correlation effects,[4] and an energy cutoff of 500 eV is set for the plane wave function's expansion. The spin-orbit coupling was also considered in the electronic structure calculations and the van der Waals (vdW) interaction between 2D layers are described by the DFT-D3 correction.[5,6] A Γ-centered k-point sampling of 3 × 3 × 2 for Brillouin zone integration are generated using the Monkhorst-Pack scheme. The lattice parameter and atomic positions of the structure is relaxed untill the total energy changes were less than 1.0×10^{-4} eV and the maximum force component acting on each atom was less than 0.02 eV Å-1.

Device fabrication and characterization: To fabricate the planar photodetectors. The interdigital Au electrodes were deposited on the surface $(PEA)_2PbBr_4$ single crystals by vacuum evaporation method via successive evaporation deposition of 150 nm Au. The spacing between neighboring fingers was controlled to be 40 μm, while the effective

illuminated area of each device was about 6×10^{-3} cm^2. The photo-response characteristics for the devices were collected by using a Keithley 4200 semiconductor characterization system and a manual probe station under various bias voltage and power density with monochromatic LED illumination (wavelength: 365 nm and 265 nm). The fast speed response characteristics of the devices were measured by an optical chopper and a Tektronix MDO 3104 Mixed Domain Oscilloscope. Besides, the irradiation was achieved by using a 375 nm semiconductor laser. Dark current noise was measured by using a spectrum analyzer (Keysight 35670A). A set of optical power meter (VEGA OPHIR PD300-UV) was used to measure the incident powers. All measurements were taken at room temperature.

Additional data and results

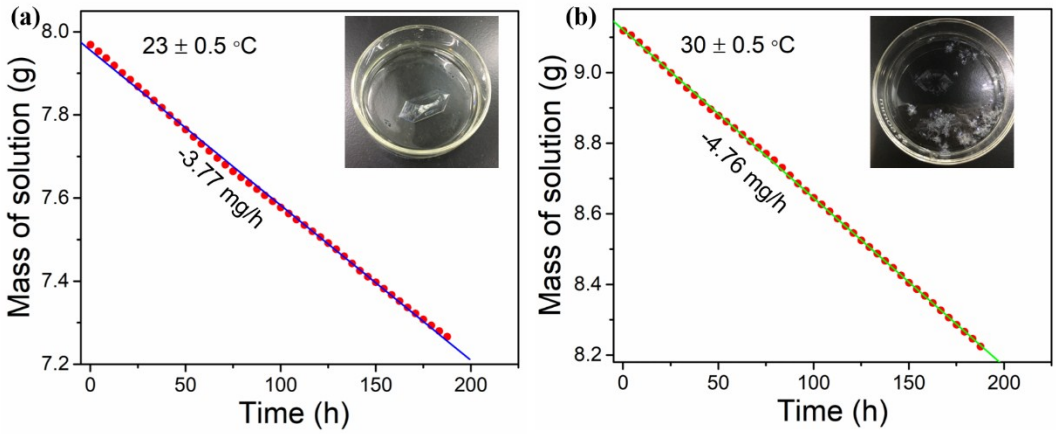

Figure S1. Mass of $(PEA)_2PbBr_4$ precursor solution as a function of evaporation time at 23 ± 0.5 °C and 30 ± 0.5 °C. Inset: The photograph of the single crystal.

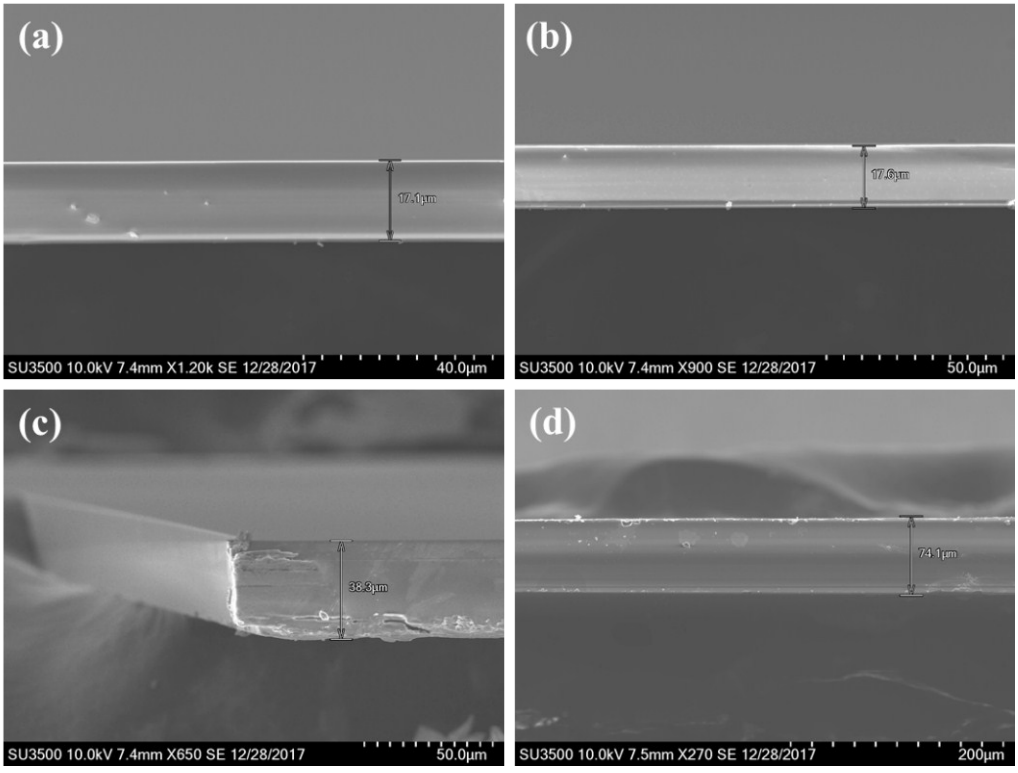

Figure S2. Cross-sectional SEM images of the $(PEA)_2PbBr_4$ single crystal with different thickness.

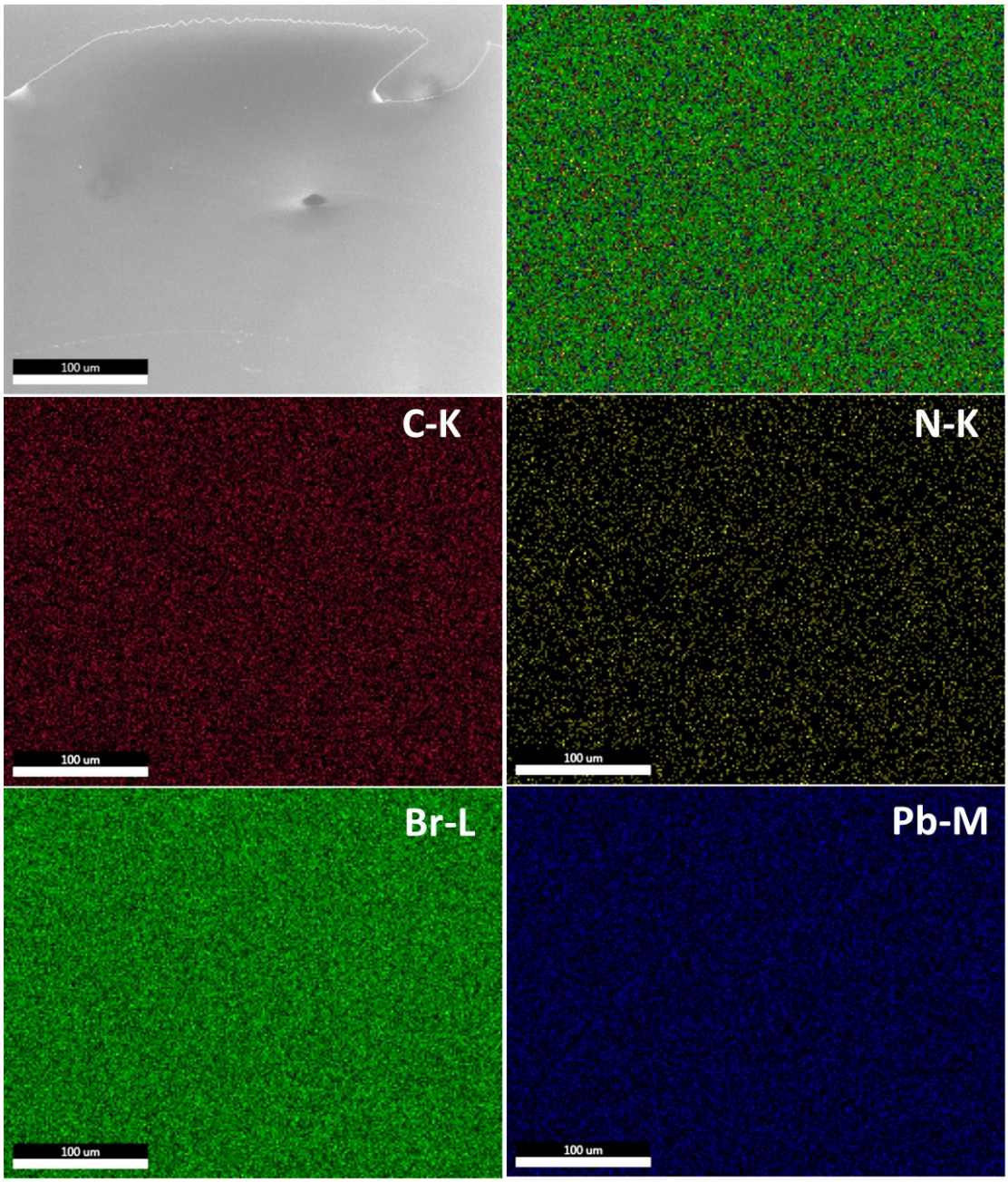

Figure S3. EDS mapping scanning measurement of the detected element C, N, Br and Pb.

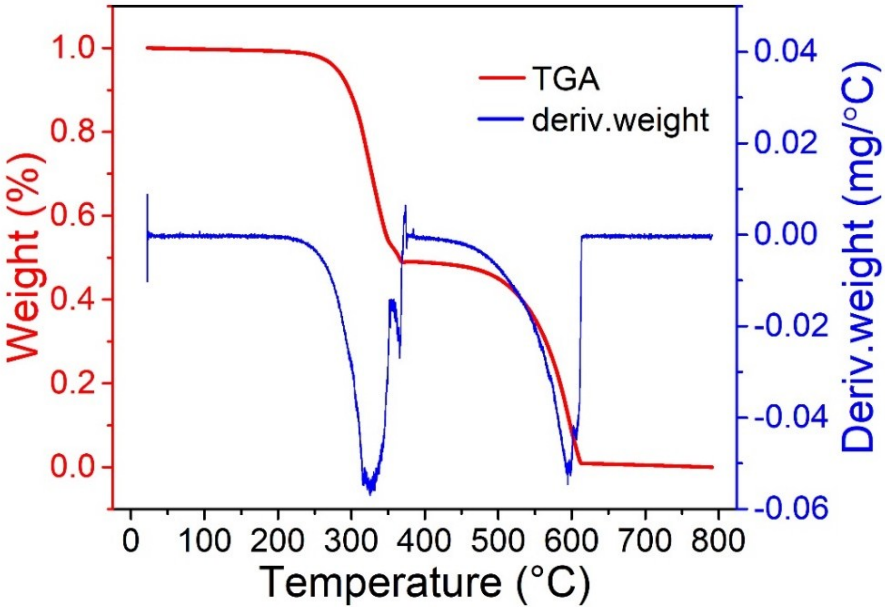

Figure S4. TGA curve and corresponding first derivative for the $(PEA)_2PbBr_4$ single crystal.

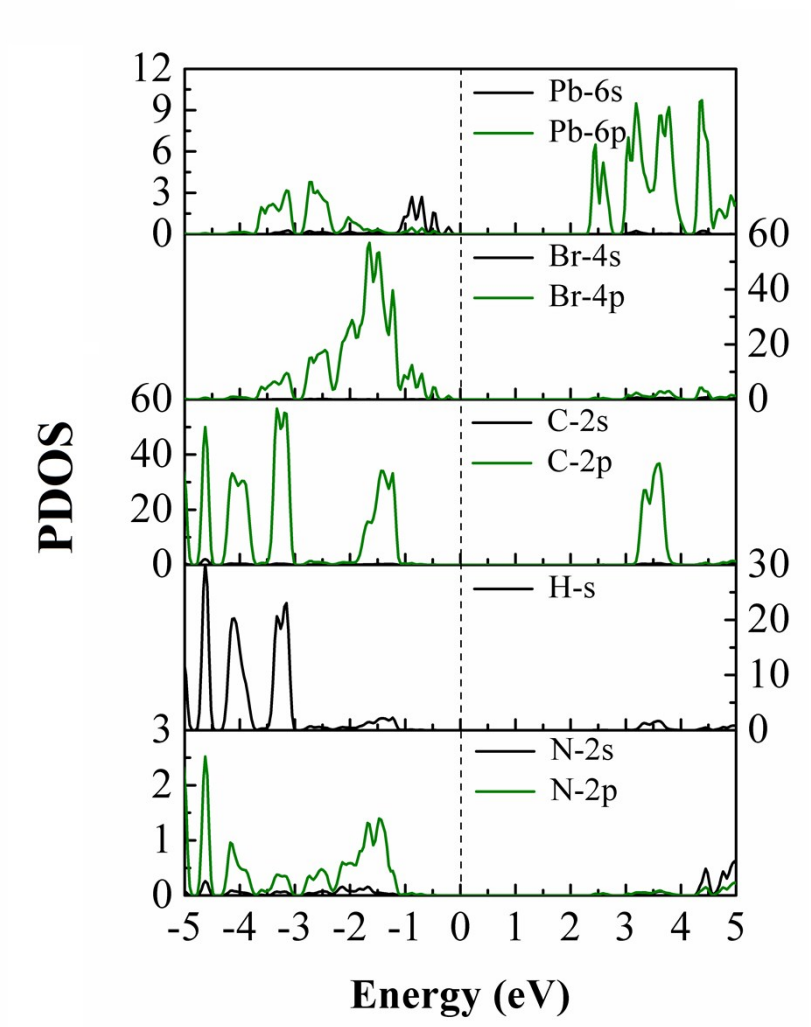

Figure S5. The partial density of states of $(PEA)_2PbBr_4$.

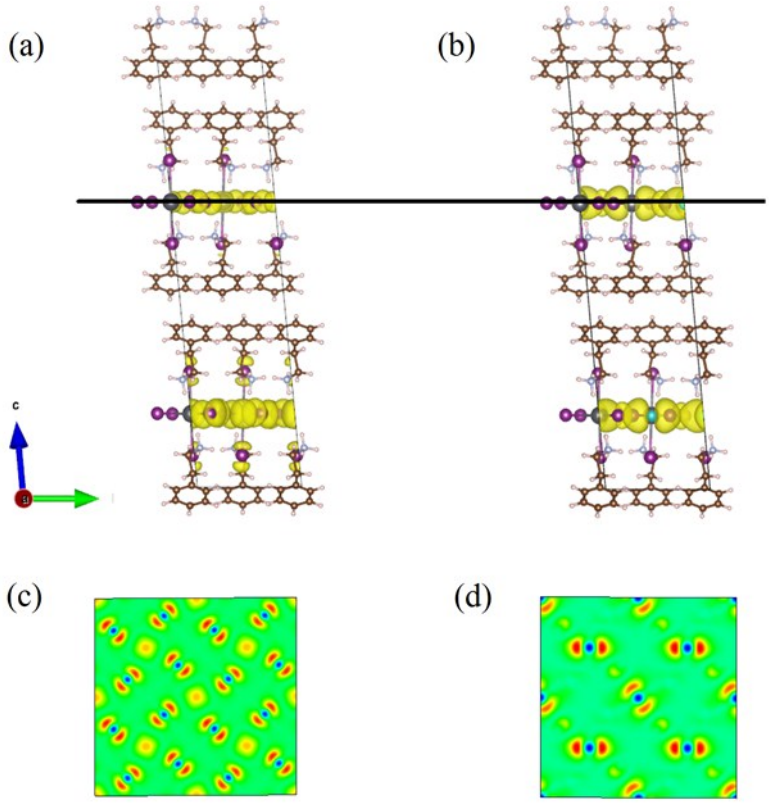

Figure S6. Side views of decomposed band charge densities of (a) VBM and (b) CBM, and their corresponding surface slice across the black line (VBM in (c) and CBM in (d)).

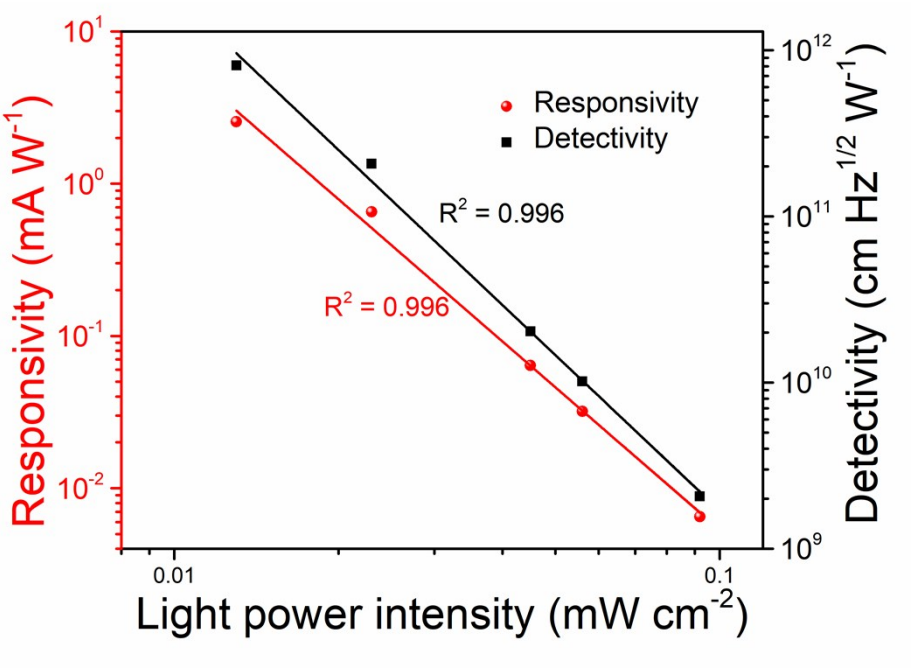

Figure S7. Responsivity and detectivity dependence on light irradiance (λ = 265 nm) for $(PEA)_2PbBr_4$ photodetector with a bias of 10 V.

Table S1. X-ray diffraction data of $(PEA)_2PbBr_4$ single crystal.

Empirical formula	$(C_6H_5C2H_4NH_3)PbBr_4$
Formula weight	771.2
Temperature	298 K
Wavelength	0.7107
Crystal system	triclinic
Space group	P-1
Unit cell dimensions	a = 11.55 α = 99.58°
	b = 11.56 β = 105.88°
	c = 17.39 γ = 89.99°
volume	2197.65
Z	4
Density (calculated)	2.27 g cm^{-3}
Absorption coefficient	14.5 mm^{-1}
F (000)	1424
Crystal size	0.3 × 0.2 × 0.02 mm3
Theta range for data coefficient	4.685-53.005°
Reflections collected	88526
Absorption correction	0.2124-0.7454
Max and min transmission	0.7454 and 0.2124
Refinement method	Full-matrix least-squares on F2
Goodness-of-fit on F^2	0.99

Table S2. Comparison of the characteristic parameters of $(PEA)_2PbBr_4$ single crystal photodetector and other UV-photodetector devices in the literatures.

Material	λ (nm)	Detectivity (jones)	dark current (nA)	Rise time	Fall time	Reference
$CH_3NH_3PbCl_3$ single crystal	365	1.2×10^{10}	415	24 ms	62 ms	[7]
ZnO thin film	380	-	-	48 s	0.9 s	[8]
TiO_2 thin film	260	-	-	6 s	15 s	[9]
ZnO nanoflakes	380	5.25×10^{10}		23 ms	26 ms	[10]
TiO_2 nanorod arrays	365	-	-	150 ms	50 ms	[11]
Si:GaN layer	365	4.87×10^{9}		29 s	141 s	[12]
Se/ZnO p-n heterojunction	370	-	-	0.69 ms	13.5 ms	[13]
ZnO/Ga_2O_3	251	6.29×10^{12}	-	0.1 ms	0.9 ms	[14]
$MAPbCl_3$ film	385	10^{12}	~1		~1 ms	[15]
$Cs_2AgInCl_6$ SC	365	10^{12}	0.01	0.97 ms	-	[16]
Graphdiyne:ZnO	365	-	-	6.1 s	2.1 s	[17]
$(PEA)_2PbBr_4$ SC	365	1.55×10^{13}	2.2×10^{-4}	0.41 ms	0.37 ms	Present work

(1) G. Kresse, J. Furthmuller, *Comput. Mater. Sci.*, 1996, **6**, 15-50.

(2) W. Kohn, L. J. Sham, *Phys. Rev.*, 1965, **140**, A1133-A1138.

(3) P. E. Blochl, *Phys. Rev. B*, 1994, **50**, 17953-17979.

(4) J. P. Perdew, K. Burke, M. Ernzerhof, *Phys. Rev. Lett.*, 1996, **77**, 3865-3868.

(5) S. Grimme, J. Antony, S. Ehrlich, H. Krieg, *J. Chem. Phys.*, 2010, **132**, 154104.

(6) S. Grimme, S. Ehrlich, L. Goerigk, *J. Comput. Chem.*, 2011, **32**, 1456.

(7) G. Maculan, A. D. Sheikh, A. L. Abdelhady, M. I. Saidaminov, M. A. Haque, B. Murali, E. Alarousu, O. F. Mohammed, T. Wu, O. M. Bakr, *J. Phys. Chem. Lett.*, 2015, **6**, 3781-3786.

(8) J. H. Jun, H. Seong, K. Cho, B.-M. Moon, S. Kim, *Ceram. Int.*, 2009, **35**, 2797-2801.

(9) H. Xue, X. Kong, Z. Liu, C. Liu, J. Zhou, W. Chen, S. Ruan, Q. Xu, *Appl. Phys. Lett.*, 2007, **90**, 201118.

(10) B. Deka Boruah, A. Misra, *ACS Appl. Mater. Interfaces*, 2016, **8**, 18182-18188.

(11) Y. Xie, L. Wei, G. Wei, Q. Li, D. Wang, Y. Chen, S. Yan, G. Liu, L. Mei, J. Jiao, *Nanoscale Res. Lett.*, 2013, **8**, 188.

(12) A. R, R. R, L. R, D. S. Vavilapalli, K. Baskar, S. Singh, *Appl. Surf. Sci.*, 2018, **435**, 1057-1064.

(13) K. Hu, F. Teng, L. Zheng, P. Yu, Z. Zhang, H. Chen, X. Fang, *Laser & Photonics Rev.*, 2017, **11**, 1600257.

(14) B. Zhao, F. Wang, H. Chen, L. Zheng, L. Su, D. Zhao, X. Fang, *Adv. Funct. Mater.*, 2017, **27**, 1700264.

(15) V. Adinolfi, O. Ouellette, M. I. Saidaminov, G. Walters, A. L. Abdelhady, O. M. Bakr, E. H. Sargent, *Adv. Mater.*, 2016, **28**, 7264-7268.

(16) J. Luo, S. Li, H. Wu, Y. Zhou, Y. Li, J. Liu, J. Li, K. Li, F. Yi, G. Niu, J. Tang, *ACS Photonics*, 2017, **5**, 398-405.

(17) Z. Jin, Q. Zhou, Y. Chen, P. Mao, H. Li, H. Liu, J. Wang, Y. Li, *Adv. Mater.*, 2016, **28**, 3697-3702.